IEICE Communications Express, Vol.13, No.8, 323–326

ComEX

LETTER

Measurement-based estimation of carrier sense behavior for simulation modeling

Ayano Ohnishi [1, a)], **Tetsuya Iye** [1], **Michio Miyamoto** [1], **and Takahito Inoshita** [1]

Abstract One possible approach to address communication delay in the complex wireless environment of manufacturing sites is to predict the delay by system-level simulator (SLS) and notify the communication control system in advance. For accurate delay prediction, the carrier sense (CS) model in SLS should incorporate real device characteristics. However, accurate modeling of CS is difficult since its implementation specifications are usually not publicly available. In this letter, we propose a method for estimating CS characteristics using electromagnetic noise generated simulatively by software-defined radio and emitted from a microwave oven and verify the effectiveness of this method.

Keywords: wireless communication, factory, electromagnetic noise, system level simulation, carrier sense, software defined radio
Classification: Sensing

1. Introduction

In recent years, the utilization of wireless systems in manufacturing settings such as factories has increased to enhance the productivity and quality of products. However, the factory environment is typically complex for wireless communication due to the prevalence of noise and interference signals. For example, industrial equipment with magnetrons, specifically microwaves, is known to generate electromagnetic (EM) noise in the ISM band, which interferes with wireless communications like wireless LAN (WLAN) operating in the 2.4 GHz band. This interference can lead to disruptions and delays in communication, potentially affecting the performance of production lines in factories where high reliability and low latency are crucial. To address this issue, we propose a communication control system designed to predict and prepare for communication delays caused by such interference. Delay estimation involves constructing models that account for the delay mechanisms within system-level simulators (SLSs) like QualNet [1], using real-world environmental data. While traffic volume and other wireless signal levels have been used to statistically determine end-to-end delay times in SLS [2]. However, estimating delay in environments with EM noise requires more comprehensive data beyond measuring MAC layer traffic.

In WLANs adopting Carrier Sense Multiple Access with Collision Avoidance (CSMA/CA) access control method, such as IEEE802.11a/b/g, delays in the MAC layer occur mainly due to the following two reasons: (1) increased demodulation failures by reduced Signal to Interference plus Noise Ratio (SINR) at the receiver due to noise and interference signals, necessitating retransmissions, and (2) postponement of transmissions when noise and interference signals are detected on the transmitter during carrier sensing before transmission. For (1), our delay prediction system utilizes a receiver model that does not return ACK signal when frame loss is determined by measured SINR and makes the transmitter retransmit the frame. Specifically, we use the SINR-to-BER (Bit Error Rate) characteristics predefined in SLS for each modulation method to determine BER from the instantaneous SINR measured at the receiver. Based on this deduced BER, frame reception is judged, and if frame loss is determined, the receiver does not return an ACK signal to the transmitter. If no ACK is returned from the receiver, the transmitter retransmit up to a maximum number of retransmissions [3]. By setting the measured power levels of EM noise in the SLS, we aim to enhance estimation accuracy by ensuring consistency between the simulation and the real environment. Meanwhile, this study focuses on (2), proposing a method to estimate carrier sense (CS) characteristics by actual measurement to improve the accuracy of delay prediction by incorporating CS characteristics of actual WLAN device into SLS. We have reported a technique that predicts delays by inputting the results of time-series predictions of EM noise [4] into an SLS that can trace the behavior of individual packets [3, 5]. To quantitatively estimate delays, it is necessary to model realistic CS characteristics in the SLS. However, the CS function of the devices, although defined in IEEE802.11-2020, is left to manufacturer implementations [6, 7]. Moreover, specifics like CS bandwidth and power threshold levels for CS are generally not disclosed, making modeling challenging. As a result, the accuracy of delay estimation may deviate from the real environment. Therefore, our study devises a method to estimate the CS bandwidth and the threshold levels by EM noise generated near the target wireless devices.

This letter is structured as follows: Section 2 discusses the estimation of CS bandwidth using simulated noise generated by software-defined radio (SDR) and CS behavior tests with practical EM noise from microwaves. Section 3 presents the experimental results and discusses CS behavior. The conclusion of our study is provided in Section 4.

[1] Kozo Keikaku Engineering Inc., 4–38–13 Hon-cho, Nakano-ku, Tokyo 164–0012, Japan
[a)] aya@kke.co.jp

DOI: 10.23919/comex.2024XBL0045
Received March 7, 2024
Accepted April 30, 2024
Publicized June 11, 2024
Copyedited August 1, 2024

2. Experimental procedure

In this study, we conduct two types of experiments: Experiment (1) estimates the CS bandwidth by generating simulated EM noise near the target wireless device using SDR. Experiment (2) uses a microwave to create EM noise with temporally varying frequency characteristics and levels to estimate the signal detection threshold levels. Details of the equipment used in experiments (1) and (2) are summarized in Table I, and the layout of the experimental setup is shown in Fig. 1, with the SDR antenna unit and microwave positioned within 30 cm of the target wireless device.

The experimental procedure in (1) is shown below. The testing method for the CS function is based on the guidelines of the "Ordinance on Technical Standards Conformity Certification of Specified Radio Equipment" stipulated by the Ministry of Internal Affairs and Communications in Japan [8]. Certification bodies conduct tests based on this ordinance, and wireless devices that pass the test are placed on the market. In the guidelines, it is recommended that if the continuous wave (CW) generated as a simulated signal cannot be detected, the frequency of the signal should be shifted or the bandwidth should be increased. In this study, following these guidelines, we test whether the transmitter can detect the noise or interference signals, i.e., whether the transmitter stops transmitting, while changing the center frequency and bandwidth of the simulated signal. To be more specific, the CW signal is initially generated at the center frequency of 2.462 GHz of the communication band (channel 11). The transmission gain was set to 65 dB (the upper setting limit for bladeRF 2.0 micro is 66 dB), a level high enough to be detectable in the WLAN station. To expand the bandwidth as a simulated noise signal, additional CW signals are emitted at fixed intervals (200 kHz) on both sides of the frequency direction from the initial CW signal.

Table I Experimental equipment specifications.

Notation	Model No.	Usage
SDR	Nuand bladeRF 2.0 micro	Noise generator
MWO	Microwave oven	Noise source
RSA	Tektronics RSA306B	Realtime spectrum analyzer
Server A	Dell Precision 3460	SDR/RSA controller
WLAN station	Wireless LAN station	Station
RPi	Raspberry Pi 4 model B 8 GB	(iperf client)
AP	Buffalo WPAM-1266R	Access point
Server B	Dospara Magnate GE i7-11700	PC (iperf server)

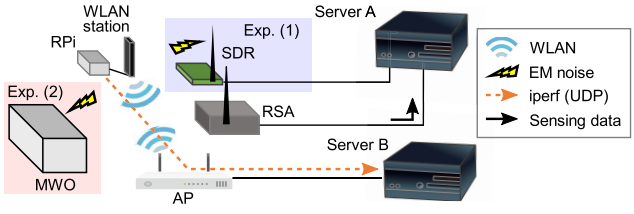

Fig. 1 Layout of the experimental equipment in the EMI shielded tent. For the experiment (1), an SDR and its antenna with blue background were used to generate EM noise, together with the equipment without color backgrounds for the experimental environment. For the experiment (2), EM noise was emitted from a microwave oven with red background color and the apparatuses without color backgrounds were also used again.

This shall be regarded as extending the effective bandwidth by approximately 400 kHz. If the noise is not sensed in the 400 kHz bandwidth, additional CW signals are added at ±400 kHz from the center to increase the effective bandwidth to 800 kHz. This process is repeated m times until the noise is sensed. Then, shift the center frequency by +0.5 MHz, keeping the effective bandwidth of $0.4m$ MHz at the time of the m-th CS. If the noise is still sensed, shift the center frequency by +0.5 MHz again. This process is repeated n times until no noise signal is sensed, resulting in a final shift of $0.5n$ MHz. Through the above process, the lower limit of the effective bandwidth corresponding to the energy to be detected as simulated noise can be checked within an error range of 0.4 MHz, and the boundary of the CS bandwidth specific to the device can be checked within an error range of 0.5 MHz. Assuming that the CS bandwidth B_{CS} [MHz] of the target device extends symmetrically from the center of the communication band, the lower and upper boundaries of B_{CS} can be estimated as shown in Fig. 2, and the following inequality constraints for the open interval can be formulated:

$$0.4 * m + n - 1.8 < B_{\mathrm{CS}} < 0.4 * m + n. \tag{1}$$

The experimental procedure in (2) is described next. EM noise generated in factories may have a wide bandwidth and time-varying frequency response. Therefore, we conducted an experiment using a common microwave oven as an interference source, which generates EM noise with a broadband frequency response in the ISM band that overlaps with the WLAN band. We estimate the detection power threshold level within the CS bandwidth, which could not be confirmed in the experiment (1) due to the lack of bladeRF output control accuracy. While operating the microwave oven at 600 W, UDP transmission by iperf was attempted from the WLAN station to the direction of the AP. At the same time, IQ (In-phase/Quadrature) samples were continuously acquired by a real-time spectrum analyzer (RSA).

Note that in this study, the Modulation and Coding Scheme (MCS) was fixed so that the automatic control of the

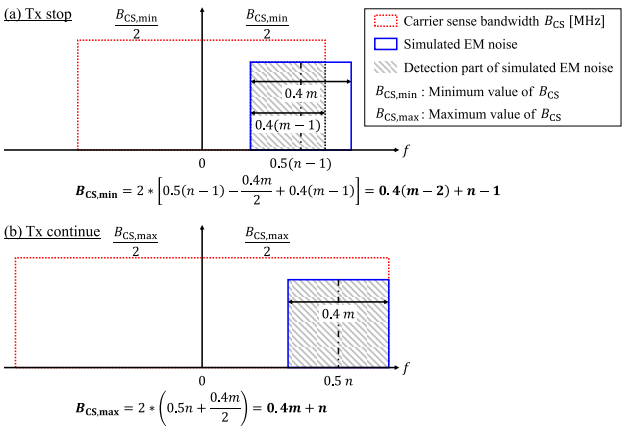

Fig. 2 (a) Illustration of estimating the lower limit of the CS bandwidth when EM noise with a bandwidth of $0.4m$ MHz is shifted $(n-1)$ times. In this case, the device sensed the noise and stopped transmission. (b) Illustration of estimating the upper limit of the CS bandwidth when EM noise with a bandwidth of $0.4m$ MHz is shifted n times. In this case, the noise could not be sensed and transmission continued. The frequency on the horizontal axis is centered at 2.462 GHz but is set to 0 MHz for simplicity.

MCS would not affect the estimation of the delay time due to variations in the signal duration during the measurement.

3. Results and discussion

The simulated noise spectrum of experiment (1) measured by RSA is shown in Fig. 3. The transmitter did not detect noise signals when the effective bandwidth was 400 kHz with three CW signals generated at 200 kHz intervals. On the other hand, expanding the effective bandwidth to 800 kHz with five signals resulted in detecting noise signals. Next, the effective bandwidth was kept at 800 kHz, and the center frequency of the simulated noise was incrementally increased by +0.5 MHz from the center frequency of the target communication band. The noise was detected up to four frequency shifts of the simulated noise, whereas when it was shifted five times and generated at +2.5 MHz from the center frequency, the noise was no longer detected. From these results, it was found that $m = 2$ is the number of steps to increase the effective bandwidth until the noise is detected, and $n = 5$ is the number of steps to shift the center frequency until the noise is no longer detected. According to the calculation procedure described in the previous section, the range of the detection bandwidth B_{CS} for the target wireless device in this study can be obtained as $4.0 < B_{CS} < 5.8$ in MHz. This suggests that the device senses noise signals within 20–30% around the center frequency for the entire 20 MHz communication bandwidth.

Next, we discuss the results of experiment (2) using a microwave oven, which was performed to confirm the CS characteristics. As shown in [4, 9, 10], the characteristic frequency of EM noise fluctuates with time. The average power of EM noise over the frequency direction shows a 10 ms period pattern consisting of a square wave or spike noise period of 20–40 us period with a constant intensity of about 7 ms and a stop period of about 3 ms. Figure 4(a-1) exhibits the case where communication continues even when EM noise overlaps the communication bandwidth. Figure 4(a-1) and Fig. 4(b-1) show the spectrograms of the RSA results for different time periods when measurements were made for 30 seconds under the same experimental conditions. Figure 4(a-2) and Fig. 4(b-2) show the received power of the signal after applying a 2 MHz low-pass filter (LPF) based on the center frequency to check the received power within the estimated minimum CS bandwidth of 4 MHz, as shown in the previous paragraph. Figure 4(a-3) and Fig. 4(b-3) show that the received power of EM noise interference is −32 dBm (> −47 dBm) within a bandwidth of 4 MHz, indicating that CS is working when the peak level of EM noise exceeds the signal power level. Figure 4(a-3) and Fig. 4(b-3) show the time-series instantaneous received power when a 10 MHz LPF is applied to confirm the received power of the entire communication band. By comparing these results with Fig. 4(a-2) and Fig. 4(b-2), it can be reconfirmed that the CS is not performed on the entire communication band but on a few MHz near the center, which supports the conclusion of the experiment (1).

Figure 4 provides a qualitative discussion. To quantitatively estimate the detection signal threshold level for CS, $P_{CS,th}$, Fig. 5 shows the measurement results before and after the EM noise level gradually decreases to below $P_{CS,th}$, and

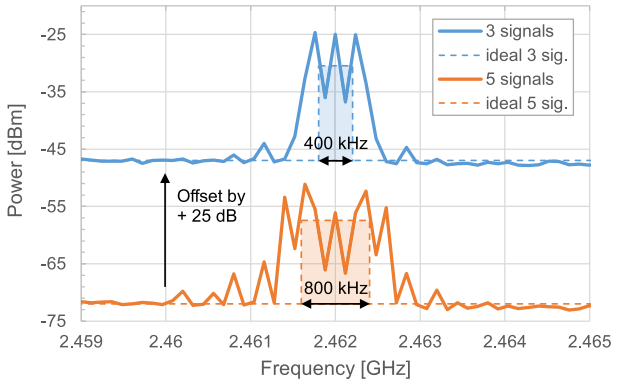

Fig. 3 Three CW signals generated at 200 kHz intervals to produce 400 kHz bandwidth simulated EM noise highlighted in light blue (blue line). Five CW signals generated at 200 kHz intervals to produce simulated EM noise with a bandwidth of 800 kHz, highlighted in light orange (orange line). The center frequency of all signals is 2.462 GHz, the center of the communication bandwidth. "3 signals" data are vertically offset by +25 dBm for clarity.

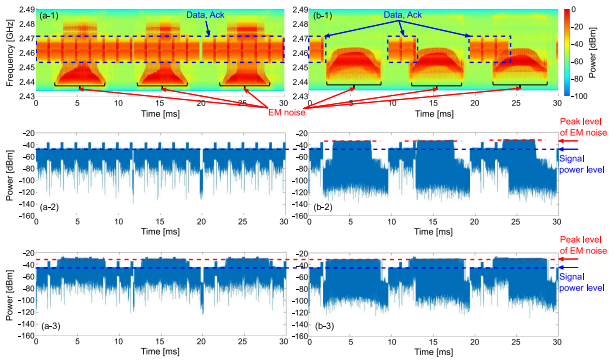

Fig. 4 Spectrograms acquired by RSA when the microwave oven was running at 600 W to generate EM noise and iperf UDP transmission from the WLAN station toward the AP. (a-1) shows the spectrogram without CS while (b-1) with CS. (a-2) and (b-2) are the time-series received power when passing through a 2 MHz LPF for the spectrograms in the upper rows, respectively. (a-3) and (b-3) are also time-series received power when the 10 MHz LPF is passed through the upper spectrogram, respectively.

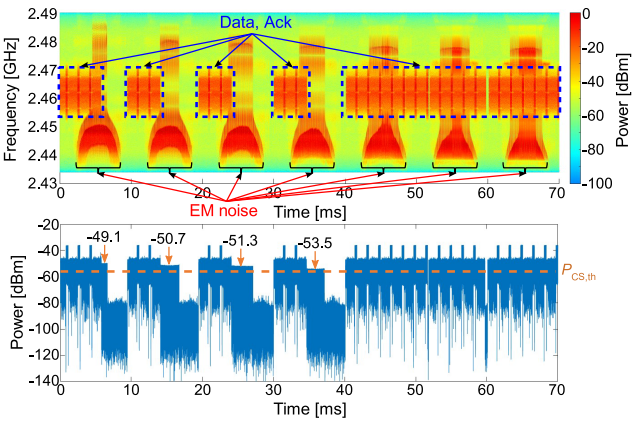

Fig. 5 (Upper figure) Spectrograms acquired by RSA when the microwave oven was running at 600 W to generate EM noise and iperf UDP transmission from the WLAN station toward the AP. (Lower figure) The received power of the EM noise gradually decreased and finally fell below the signal detection threshold level $P_{CS,th}$, which is why the signal was continued in the second half of the transmission.

transmission is no longer stopped. The received level of EM noise within the CS bandwidth of 4 MHz extracted by applying a 2 MHz LPF decreased every 10 ms to −49.1 dBm, −50.7 dBm, −51.3 dBm, and −53.5 dBm, and no noise was sensed after 40 ms. The rate of change in received EM noise power is about −147 dB/s for the first 40 ms. Simple linear extrapolation from the rate of change in the first half suggests that the EM noise was about −55 dBm at 45 ms. At this moment, the received power −55 dBm is below $P_{\mathrm{CS,th}}$ and is no longer sensing noise. From this result, it can be inferred that the CS of the target device adopts a value of $P_{\mathrm{CS,th}}$ [dBm] within a bandwidth of 4 MHz in range of $-55 < P_{\mathrm{CS,th}} < -53.5$ on the measurement scale by RSA.

The CS bandwidth and detected signal threshold levels estimated in experiments (1) and (2) can be set as EM noise CS conditions within the SLS to support future realistic and accurate delay estimation. In addition, as mentioned previously, the details of the CS operating specifications are implementation-dependent for the manufacturer and are basically not disclosed. To investigate the impact of differences in CS implementation specifications on communication delay, it is necessary to clarify the differences in CS for each wireless device as future work and reflect them as variations in the simulation model.

4. Conclusion

In this study, we developed a methodology for measuring and estimating carrier sense (CS) behavior in wireless communication systems, particularly in manufacturing factories with electromagnetic (EM) noise. Through experiments using both synthetic and real-world EM noise sources, we established a framework for estimating CS characteristics that significantly affect communication delay. Our experiments quantitatively estimated the CS function of the target wireless device senses noise when the noise power level exceeds −54 dBm within 4.0 to 5.8 MHz, equivalent to 20–30% of the entire 20 MHz bandwidth, near the central frequency of the 2.4 GHz WLAN communication band in the presence of EM noise. This insight is crucial for refining delay estimations in system-level simulators, enhancing the reliability of wireless communications in industrial environments with variable noise conditions. Further research should focus on diversifying simulation models to account for the variability in device-specific CS implementations, which remains largely undisclosed by manufacturers, to refine delay predictions and support the robust design of wireless networks.

Acknowledgments

This work is supported by the Ministry of Internal Affairs and Communications as part of the research program “R&D for Expansion of Radio Wave Resources (JPJ000254)”.

References

[1] Keysight Technologies, “Network modeling,” https://www.keysight.com/us/en/products/network-test/network-modeling.html, accessed Feb. 29 2024.

[2] A. Kashyap, S. Ganguly, and S.R. Das, “Measurement-based approaches for accurate simulation of 802.11-based wireless networks,” Proceedings of the 11th International Symposium on Modeling, Analysis and Simulation of Wireless and Mobile Systems (MSWiM ’08), New York, NY, USA, pp. 54–59, 2008. DOI: 10.1145/1454503.1454516

[3] N. Ohuchi, T. Oota, and T. Inoshita, “Delay time prediction technology for delay guarantee – a study on utilization of physical measurement data in system level simulation,” The 2022 IEICE General Conference, B-17-21, 2022 (in Japanese).

[4] T. Iye, A. Ohnishi, S. Okuno, M. Miyamoto, and T. Inoshita, “Background traffic forecasting using extreme learning machine for delay guarantee,” 2024 IEEE International Conference on Consumer Electronics (ICCE), Las Vegas, NV, USA, pp. 1–4, 2024. DOI: 10.1109/ICCE59016.2024.10444157

[5] T. Inoshita, T. Oota, N. Ohuchi, and O. Kiriyama, “Delay time prediction technology for delay guarantee – development of prediction system based on wireless communication environment measurement and system level simulation,” The 2022 IEICE General Conference, B-17-20, 2022 (in Japanese).

[6] J. Bailey, S. Liu, I. Lambadaris, S. Max, and D. Sugirtharaj, “Survey of commercial Wi-Fi devices’ energy detection mechanism,” 2024 IEEE International Conference on Consumer Electronics (ICCE), Las Vegas, NV, USA, pp. 1–6, 2024. DOI: 10.1109/ICCE59016.2024.10444169

[7] “IEEE Standard for Information Technology–Telecommunications and information exchange between systems - local and metropolitan area networks–specific requirements - part 11: wireless LAN medium access control (MAC) and physical layer (PHY) specifications,” IEEE Std 802.11-2020 (Revision of IEEE Std 802.11-2016), 2021. DOI: 10.1109/IEEESTD.2021.9363693

[8] Ministry of Internal Affairs and Communications, “Ordinance on technical standards conformity certification of specified radio equipment,” Appended table 43 (Article 2, paragraph (1), item (xix)).

[9] A. Ohnishi, M. Miyamoto, Y. Takeuchi, T. Maeyama, A. Hasegawa, and H. Yokoyama, “Electromagnetic wave pattern detection using cepstral features in the manufacturing field,” IEICE Commun. Express, vol. 9, no. 12, pp. 650–655, 2020. DOI: 10.1587/comex.2020COL0039

[10] A. Ohnishi, M. Miyamoto, Y. Takeuchi, T. Maeyama, A. Hasegawa, and H. Yokoyama, “Electromagnetic wave pattern detection with multiple sensors in the manufacturing field,” IEICE Trans. Commun., vol. E106-B, no. 2, pp. 109–116, 2023. DOI: 10.1587/transcom.2022CEP0005